

Current Distribution in Exciting Coil Conductors in Cross-Field Heating Systems

K.V.Namjoshi and P.P.Biringer

Department of Electrical Engineering, University of Toronto,
Toronto, Ontario, M5S 1A4, Canada.

Abstract -In this paper, we analyze the current distribution in the exciting coils of double sided iron backed cross-field heating systems. Finite difference method is used to calculate the internal resistance of the winding. Using the internal resistance as a criterion, the effect of the load on the winding current distribution is studied. Concept of equivalent surface current density is introduced to show the influence of the parameters such as the winding cross section and the skin depth. Equivalent surface current density is obtained by placing virtual current sources at the interface of the winding conductor and the air gap. Impedance values calculated using the two methods are in agreement.

I. INTRODUCTION

Cross-field heating systems are commonly used for the heat treatment of thin plates and sheets[1]. Here, the winding conductors are embedded in slots of high permeability backing iron. These arrangements differ from that of electric machines in that the frequency of operation is about a few kHz or higher and the air gap is larger (about a few inches). The induced power in the load or the workpiece depends on the incident field which is a function of the current distribution in the winding conductors. In addition, the winding power loss also depends on the current distribution. Therefore, the dependence of the conductor internal resistance and reactance on the winding current distribution is of interest. In the past, current distribution in conductors embedded in high permeability core has been obtained by placing certain restrictions on the magnetic field at the entrance of the slot[2-4]. In an earlier paper, we have presented a calculation of the induced load power and its dependence on parameters such as the operating frequency and the electrical properties of the load[5]. In this paper, we investigate the load dependence of the winding current distribution in iron backed double sided cross-field heating systems. Change in the internal resistance of the winding is used as an indication of the change in the current distribution in the winding. Finite difference method is used. A periodic arrangement is assumed and a two dimensional model is used. The permeability of the iron backing is assumed to be infinity. Numerical results are presented for the winding resistance and reactance for a few load conditions. To study the influence of parameters such as the conductor cross section and the skin depth on the current distribution, concept of equivalent surface current density is introduced. Equivalent surface current density is obtained under

the no load condition by placing virtual current sources at the boundary between the conductor and the air gap. A comparison is given of the winding impedance obtained by the two methods.

II. CURRENT DENSITY AND INTERNAL RESISTANCE

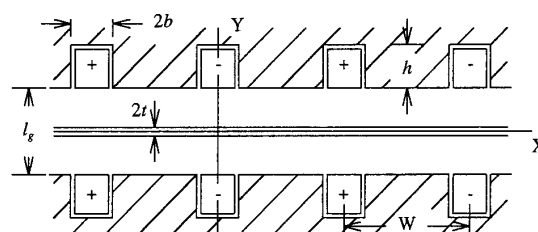


Figure 1: A cross-field heating system with double sided iron backing showing the winding conductors in the slots and the load.

A schematic diagram of a double sided cross-field heating system with a periodic arrangement of slots is shown in Fig.1. Its dimension in the Z direction is assumed to be very large, i.e., the system is assumed to be two dimensional. The conductors have the same cross section as that of the slots ($h \times 2b$). The exciting coils carry current in the Z direction. Therefore, the magnetic vector potential and the induced current density have non zero components only in the Z direction.

To obtain the vector potential A_Z and the current density J_Z , the following field equations are solved in the region of interest:

In the slot conductors:

$$\nabla^2 A_Z - k_c^2 A_Z = -\mu_0 \sigma_c E_D, \quad (1)$$

in the air gap:

$$\nabla^2 A_Z = 0 \quad (2)$$

and in the workpiece:

$$\nabla^2 A_Z - k_w^2 A_Z = 0. \quad (3)$$

$$k_c = \sqrt{j\omega\mu_0\sigma_c} = (1+j)/\delta_c$$

$$\text{and } k_w = \sqrt{j\omega\mu_R\mu_0\sigma_w} = (1+j)/\delta_w.$$

Here, σ_c is the conductivity of the slot conductors, σ_w the conductivity of the workpiece, μ_R the relative permeability of the workpiece, μ_0 the permeability of the free space, ω the supply frequency, δ_c the skin depth in the winding conductors, δ_w the skin depth in the workpiece and E_D is the voltage drop across the winding conductors. The current density in the winding conductors, J_{cz} , and the conductor current, I , are given by

$$J_{cz} = \sigma E_D - k_c^2 A_z / \mu_0 \quad (4)$$

$$\text{and } I = \int_{\text{cross section}} J_{cz} ds. \quad (5)$$

Equations (4-5) yield X_L , the conductor reactance per unit length and R_T , the total conductor resistance per unit length as

$$R_T + X_L = E_D / I \quad (6)$$

$$R_T = R_c + R_R.$$

R_R is the reflected resistance per unit length which depends on the load. R_c is the internal resistance per unit length. Its dependence on J_{cz} and P_c , the internal power loss per unit length, is obtained by:

$$P_c = \frac{1}{\sigma_c} \int_{\text{cross section}} J_{cz}^2 ds = I^2 R_c. \quad (7)$$

The total power per unit length of the conductor, P , is obtained from the knowledge of the conductor current I .

$$P = \text{Re}(E_D \times I^*). \quad (8)$$

The field equations are solved using the finite difference method(FDM). The symmetry of the system is taken into account.

Calculations

R_c and X_L are calculated (6-7) for a set of dimensions at several load conditions and the results are given in Tables I and II. R_c does not change significantly with the changes in the load.

TABLE I: CONDUCTOR RESISTANCE($m\Omega/m$).
 $l_s=2''$, $W=6''$, $b=0.625''$, $h=1.25''$, $f=3000\text{Hz}$ and $\delta_c=0.0012m$.

	R_c	R_R	R_T	X_L
no load	0.72	0.0	0.72	34.68
$\mu_R=1$ $\delta=0.01m$	0.70	6.89	7.59	13.59
$\mu_R=1$ $\delta=0.012m$	0.67	0.18	0.85	10.99
$\mu_R=100$ $\delta=0.001m$	0.71	7.91	8.63	17.81

TABLE II: CONDUCTOR RESISTANCE($m\Omega/m$).
 $l_s=2''$, $W=6''$, $b=0.25''$, $h=0.5''$, $f=3000\text{Hz}$ and $\delta_c=0.0012m$.

	R_c	R_R	R_T	X_L
no load	1.13	0.0	1.13	40.96
$\mu_R=1$ $\delta=0.01m$	1.19	4.28	5.47	17.01
$\mu_R=1$ $\delta=0.012m$	1.18	0.14	1.32	15.66
$\mu_R=100$ $\delta=0.001m$	1.23	1.83	3.06	44.68

III. EQUIVALENT SURFACE CURRENT DENSITY

Since the winding current distribution does not change significantly with the load, one may use the current distribution obtained under the no load condition to estimate the incident air gap field. It may then be used to obtain quantities such as the induced load power[6]. Towards this goal, we introduce a concept of the equivalent surface current density. It is the surface current density, which, when placed on a plain backing, produces the same field in the air gap as that produced by the system of Fig.1. It is calculated using the method described below.

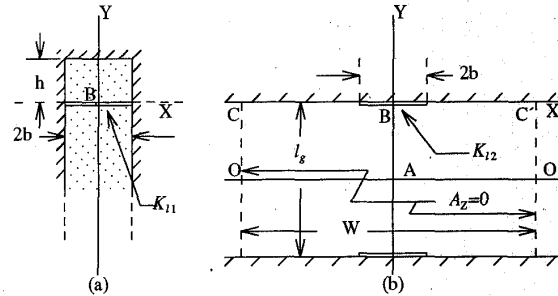


Figure 2: (a) A semi-unbounded slot filled with conductor, (b) an air gap without the slot, and the accompanying current densities, K_{11} and K_{12} .

As shown in Fig.2, the slot-airgap configuration is replaced by two regions: a) a semi-unbounded slot filled with the conductor and b) the air gap without the slot. The load is absent. The current density in the slot is expressed as:

$$J_{cz} = \frac{Ik_c}{2b} \frac{\cosh k_c(Y-h)}{\sinh k_ch}. \quad (9)$$

Here, I is the current enclosed in the region ($Y=h$ to $Y=0$) of the conductor of Fig.2a. Equation (9) satisfies the boundary conditions every where except at $Y=0$. At $Y=0$, the interface of the conductor and air gap adds to the current density a component which is a function of X . The effect of the air-conductor interface is taken into account by introducing equivalent surface current densities K_{11} in the conductor

region and K_{12} in the air gap as shown. These have an even symmetry with respect to X . The interface does not change the total current in the conductor. Therefore,

$$\int_0^b K_{11} dX = 0. \quad (10.a)$$

$$\text{and } \int_0^b K_{12} dX = \frac{I}{2}. \quad (10.b)$$

Now, we have near $Y=0$,

in the conductor

$$H_X \text{ (at } Y=0_+) = -K_{11}/2 + \frac{I}{2b}, \quad (11.a)$$

$$H_X \text{ (at } Y=0_-) = K_{11}/2 + \frac{I}{2b}, \quad (11.b)$$

and in the air gap,

$$H_X \text{ (at } Y=0_-) = K_{12}. \quad (12.a)$$

$$H_X \text{ (at } Y=0_+) = 0. \quad (12.b)$$

Because of the iron backing, there is no field at $Y=0_+$ (Fig.2b). One can write (11) only because K_{11} has no average component (10). The condition that the tangential component, H_X is continuous at the boundary, leads to

$$\frac{I}{2b} - \frac{1}{2} K_{11} = K_{12}. \quad (13)$$

K_{11} and K_{12} are divided into $(M+1)$ discrete current elements each. M is an integer. From (10) and (13) it follows that we have only M unknowns. The contribution to the vector potential by each of the current elements is obtained in terms of Green's functions corresponding to the geometry under consideration (Fig.2). In the air gap region, the Green's function is obtained using the following conformal transformation[7].

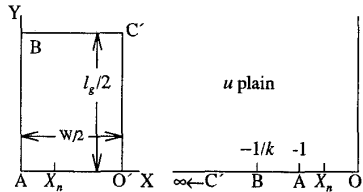


Figure 3: Transformation to obtain Green's function for the air gap region.

$$u = -\frac{cn(m(X+jY), k)}{dn(m(X+jY), k)} \quad (14)$$

$$u_n = -\frac{cn(mX_n, k)}{dn(mX_n, k)} \quad (15)$$

$$A_Z \text{ due to } I_{2n} = \frac{\mu_0 I_{2n}}{2\pi} \log \left| \frac{u+u_n}{u-u_n} \right|. \quad (16)$$

$$m = \frac{K(k)}{W/2} = \frac{K'(k)}{l_g/2} \quad (17)$$

$$\text{and } K(k) = \int_0^1 \frac{dx}{\sqrt{1-x^2} \sqrt{1-k^2 x^2}}. \quad (18)$$

cn and dn are elliptic functions[8], k is chosen such that:

$$K(k)/K'(k) = W/l_g. \quad (19)$$

I_{2n} is the current in element 'n' at location $(X_n, 0_-)$ in the air gap. When k is close to unity, i.e., $W > 2.5l_g$, one may use the following approximate expression for A_Z :

$$A_Z \text{ due to } I_{2n} = \frac{\mu_0 I_{2n}}{2\pi} \log |\sinh m(X+jY) - \sinh(mX_n)|. \quad (20)$$

In the conductor region, i.e. in the slot, the contribution to the vector potential can be expressed as

$$A_Z \text{ due to } I_{1n} = \frac{\mu_0 I_{1n}}{2\pi} K_0(k_c \sqrt{(X-X_n)^2 + Y^2}). \quad (21)$$

K_0 is the modified Bessel function of the second kind and of order zero. I_{1n} is the current at location $(X_n, 0_+)$ in the metal. In addition, one must take into account the contribution due to images formed by the slot boundaries. The current elements are determined by equating H_Y , i.e., the normal component of the magnetic field, at M locations interspersed between the $(M+1)$ locations of the current elements. K_{12} , thus obtained, is then used to predict the winding impedance. The voltage drop across the conductor is related to the total flux produced. The flux in the air gap is obtained by the vector potential at location B produced by K_{12} . The field at the surface of the conductor ($Y=0_+$) yields the internal flux of the conductor. Therefore,

$$E_D = j\omega(\text{Air gap flux}) + \frac{Ik_c}{2b\sigma_c} \frac{\cosh k_c h}{\sinh k_c h} \quad (22)$$

$$= I(R_c + X_L). \quad (23)$$

Here, it should be remembered that (23) gives impedance under no load. Since the calculations are needed only at the interface, this method is faster than the difference method or any other method which requires calculations over the entire area of the conductor.

Calculations

Integrated current, i.e., K_{12} integrated along the width of the conductor (Fig.2), is shown in Fig.4 for two cross sections. Fig.5 shows current density for different values of the skin depth of the winding conductor.

$$\text{Integrated current} = \int_0^x K_{12} dx. \quad (24)$$

Also shown in Fig.4 is the current density calculated analytically assuming $\sin^{-1}(X)$ dependence. Impedance values calculated by using (23-24) are given in Table III.

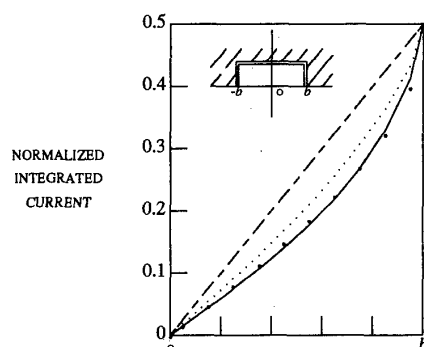


Figure 4: Effective integrated current along the conductor half width. Solid line - $b=0.625$ ", dotted line - $b=0.25$ ". The dashed line shows the result for the uniform current density and the solid circles represent the result of $\sin^{-1}(X)$ distribution. $l_g=2$ ", $W=6$ ", $h=2b$ and $\delta_c=0.0012m$.

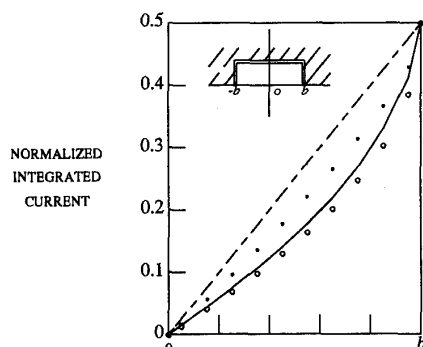


Figure 5: Effective integrated current along the conductor half width. Solid line - $\delta=0.0012m$, circles - $\delta=0$ and dots - δ large. The dashed line shows result for the uniform current density. $l_g=2$ ", $W=6$ ", $h=1.25$ " and $b=0.625$ ".

TABLE III: CONDUCTOR REACTANCE AND RESISTANCE ($m\Omega/m$) BY TWO METHODS. $f=3000Hz$, $l_g=2$ ", $W=6$ " and $\delta_c=0.0012m$.

b		FDM	Virtual source
0.625"	R_c	0.72	0.82
0.625"	X_L	34.68	35.28
0.25"	R_c	1.13	1.54
0.25"	X_L	40.96	44.17

The resistance values calculated by the both methods, though agree for the wider conductor ($=1.25$ "), show significant difference for the narrower conductor ($=0.5$ "). In the latter case, the agreement may be improved by selecting a finer mesh for the FDM.

IV. CONCLUSIONS

The equivalent surface current density can be obtained relatively easily under the no load condition. It may then be used to estimate the incident air gap field and the winding impedance. Once the incident field is known other quantities such as the workpiece power can be obtained by any of the available methods[9].

REFERENCES

- [1] S.B.Lasday, "Work progressing for continuous annealing of sheet by transverse flux induction heating at steel plant", *Industrial Heating*, October, 1991, p.43-45.
- [2] A.Konrad et al., "Finite element analysis of steady state skin effect in a slot embedded conductor", *IEEE Power Engineering Society Winter Meeting*, Jan 25-30, 1976, p.A-76-189-1.
- [3] W.Fritz, "Eddy currents in slot bars - a critical view", *ETZ Arch.(Ger.)* vol.12,no.10, 1991, p.321.
- [4] R.Palka and M.Ziolkowski, "Analysis of current density distribution in bars placed in a slot", *Arch. Electrotech.(Ger.)* vol. 64, no.3-4, 1981, p.143.
- [5] K.V.Namjoshi and P.P.Biringer, "General properties of cross-field heating systems", *IEEE Trans. Mag.*, vol.23(1987), p.3023-3025.
- [6] K.V.Namjoshi and P.P.Biringer, "Cross-field heating systems: Influence of system parameters", *IEEE Trans. Mag.*, vol.25(1989), p.3254-3256.
- [7] F.Bowman, *Introduction to Elliptic Functions with Applications*, Dover, New York(1961), p.47-49.
- [8] P.M.Morse and H.Feshbach, *Methods of Theoretical Physics*, McGraw-Hill, New York(1953), p.487.
- [9] See for example S.R.H.Hoole, *Computer-Aided Analysis and Design of Electromagnetic Devices*, Elsevier, New York(1989).

P.P.Biringer has Dip.Eng. from the Technical University of Budapest. Budapest, Hungary, M.Sc. from the Royal Institute of Technology, Stockholm, Sweden and Ph.D. from the University of Toronto, Toronto, Canada. He is currently Professor Emeritus of Electrical Engineering at the University of Toronto. He is a Fellow of the IEEE.

K.V.Namjoshi has B.E. and M.E. in Electrical Communication Engineering from the Indian Institute of Science, Bangalore, India and Ph.D. in Electrical Engineering from the University of Rhode Island, Kingston, USA. Presently, he is associated with the Electrical Engineering Department of the University of Toronto, Toronto, Canada.